Tellus (1996), 48B, 583–600
Printed in UK – all rights reserved

TELLUS
ISSN 0280–6509

A globally aggregated reconstruction of cycles of carbon and its isotopes

ATUL K. JAIN[1]*, HAROON S. KHESHGI[2] and DONALD J. WUEBBLES[1], [1]*Department of Atmospheric Sciences, University of Illinois, Urbana, IL 61801, USA;* [2]*Exxon Research and Engineering Company, Annandale, NJ 08801, USA*

(Manuscript received 30 November 1995; in final form 3 May 1996)

ABSTRACT

A globally aggregated model of the carbon cycle with an upwelling/diffusion ocean and a 6-box biosphere is developed to consistently reconstruct the carbon cycle and isotopic variation in the atmosphere and oceans. The calculated atmospheric $\delta^{13}C$ trend, based on a model that reproduces the CO_2 concentration record, agrees well with the observed ice core and tree-ring $\delta^{13}C$ records. The model has also been used to estimate the $\delta^{13}C$ of oceanic dissolved inorganic carbon, and our model results match observations well within the range of observational uncertainty. This model is found to also match measured values (within measurement error) of the pre-bomb decrease in ^{14}C in the atmosphere and the mixed layer due to the *Suess Effect*, the bomb-^{14}C in the mixed layer, the bomb-^{14}C penetration depth, the bomb-^{14}C ocean inventory, and the vertical distribution of total dissolved carbon and ^{14}C. In addition, the model is used to close the balance between the rates of increase of global inventory and of bomb production of radiocarbon. Our confidence in both the global aggregation of data and our understanding of global carbon cycle is strengthened by the consistency between carbon isotope concentration data and model results.

1. Introduction

The emission of carbon dioxide to the atmosphere by the burning of fossil fuels and changes in land use has led to an increase in the atmospheric concentration of carbon dioxide, a greenhouse gas, which can effect the global climate. However, the ability to predict how the carbon cycle responds to the emission of carbon dioxide, changes in land use, and changes in climate, relies on the understanding of the global carbon cycle, which stems from the ability to describe pertinent carbon cycle mechanisms and the measured behavior of the past carbon cycle.

In studies of global carbon cycle, models are used to apply the understanding of carbon cycle mechanisms to the prediction of the atmospheric concentration of carbon dioxide. The dissolution of CO_2 in the oceans and the incorporation of CO_2 in the terrestrial biosphere are thought to be the primary sinks of CO_2 emitted to the atmosphere over time scales of decades to centuries. While detailed understanding of these processes adds to the ability to describe the carbon cycle, this understanding is incomplete. Therefore, carbon cycle models rely on the observed behavior of past changes in the carbon cycle to calibrate or test the model's ability to represent the carbon cycle. Models are then applied under the assumption that the carbon cycle behaves according to the combined understanding of detailed yet incomplete description of the pertinent mechanisms and measurable past behavior.

There are three isotopes of carbon (^{12}C, ^{13}C and

* Corresponding author:
email: jain@atmos.uiuc.edu

^{14}C) present in the atmosphere, the terrestrial biosphere and the oceans that are useful in interpreting the behavior of carbon cycle. The small size of the global ocean and terrestrial carbon sinks relative to the precision with which the globally aggregated size of the ocean and terrestrial biospheric carbon reservoirs can be surveyed is a barrier to the direct measurement of the carbon sinks. We resort to the interpretation of measurable changes in isotopic concentrations in the oceans and atmosphere to infer the size of carbon sinks and to check the consistency with carbon cycle models.

The atmospheric ratios of ^{13}C to ^{12}C have exhibited measurable variations in both space and time. The ^{13}C ratio differs between the atmosphere, oceans, the biosphere, and fossil fuels. The primary factor causing this isotopic variability is the fractionation of ^{13}C relative to ^{12}C during certain biological transformations of compounds containing carbon. A classic example of an isotopically selective process is photosynthesis where CO_2 along with inorganic nutrients are consumed by plants to form organic compounds. This process discriminates against ^{13}C resulting in organic carbon that is significantly depleted in ^{13}C relative to the atmosphere or ocean reservoirs from which the carbon originates. Respiration (the reverse process of photosynthesis where organic carbon is metabolized to CO_2) is largely non-isotopically selective. This means that respired CO_2 has an isotopic abundance that is very similar to the $^{13}C/^{12}C$ ratio of the organic carbon substrate, and therefore is also depleted in ^{13}C with respect to atmospheric CO_2. Fossil fuels retain the isotopic composition of the ancient organic carbon of which they are made. The burning of fossil fuels releases CO_2 to the atmosphere that has a low $^{13}C/^{12}C$ similar to respired biospheric carbon. Thus, the history of $^{13}C/^{12}C$ isotope ratio of the atmospheric carbon can be partially related to changes in the size of, and exchange rate between, the various terrestrial carbon reservoirs, and CO_2 emission from the burning of fossil fuel. At the same time, ^{13}C isotope is fractionated to a lesser extent during the formation of calcite ($CaCO_3$) in the oceans. The variation in the ratio of $^{13}C/^{12}C$ throughout the ocean can be used to indicate the relative importance of the above processes in the distribution of carbon in the oceans.

Radiocarbon, the ^{14}C isotope with a half-life of 5730 years, is present in atmospheric CO_2 with a $^{14}C/^{12}C$ ratio of about 10^{-12}. Over time scales of thousands of years, radiocarbon lost from the atmosphere by radioactive decay or transfer to the oceans or to the biosphere is replenished by the generation of radiocarbon in the upper atmosphere by cosmic radiation. Ancient carbon sequestered in fossil fuels, however, contains virtually no radiocarbon. The detection of the dilution of atmospheric ^{14}C caused by fossil fuel emission of CO_2 by Suess (1955) showed the potential which ^{14}C-analysis holds for studies of the carbon cycle and its response to perturbations. There are two other ways in which radiocarbon can also serve as a useful tracer of *ocean* carbon uptake. First, the radiocarbon abundance in the deep ocean water indicates the length of time the ocean water has been prevented from exchanging carbon with the atmosphere, and is used to infer the behavior of deep ocean circulation. Second, the measurable change in ocean radiocarbon concentration caused by radiocarbon produced in the atmosphere during the era (1950 to 1963) of atmospheric nuclear weapons testing can be used to infer the extent of the transport of carbon in the upper kilometer of the oceans. It has been hypothesized (Broecker et al., 1980) that models capable of reproducing the distribution of bomb-produced radiocarbon in the oceans will also be capable of predicting the uptake of anthropogenic CO_2 because both have a similar characteristic time scale ($\approx$20 yr). These characteristics of the radiocarbon distribution provide a means of testing the validity of models that simulate air-sea exchange of CO_2 and the transport of carbon-containing molecules in the ocean.

There has been a history of studies that have made use of comparisons to data on CO_2, ^{13}C and ^{14}C concentrations in the atmosphere and oceans to calibrate or check our understanding of changes in the carbon cycle over the past century. Globally aggregated models (Oeschger et al., 1975; Broecker et al., 1980; Enting and Pearman, 1987; Siegenthaler and Oeschger, 1987; Siegenthaler and Joos, 1992; Broecker and Peng, 1994; Hesshaimer et al., 1994; Shaffer and Sarmiento, 1995; Jain et al., 1995) have been used to compare to global mean data for the atmosphere and depth dependent data for the oceans. Spatial variations of isotopic ratios of carbon have been used as a check on three-dimensional ocean tracer models

(Maier-Reimer and Hasselmann, 1987; Sarmiento et al., 1992; Maier-Reimer, 1993). Spatial gradients in atmospheric composition have been used to infer the spatial distribution of sources and sinks (Keeling et al., 1989; Tans et al., 1990; Cias et al., 1995).

In this study we apply a self-consistent model for globally-aggregated cycles of ^{12}C, ^{13}C and ^{14}C. The model contains nine carbon reservoirs, including a depth-dependent ocean. This model has been used to reconstruct the past carbon budget (Kheshgi et al., 1996), analyze future scenarios for carbon emissions (Jain et al., 1994b), and results have been compared with other carbon cycle models (Enting et al., 1994). We present in this paper a model-estimated pre-anthropogenic steady-state and transient reconstruction of past distributions of carbon and its isotopes, which are governed by the transport, fractionation, and radioactive decay processes discussed above along with estimates of emissions from fossil fuel burning and changes in land use. We also compare the model reconstruction of the past cycles of ^{12}C, ^{13}C and ^{14}C to currently-available historical record of global-mean data for the atmosphere and depth-dependent data for the oceans.

2. Model description

A nine-reservoir model of the global carbon cycle has been developed to estimate the isotopic anomaly in the atmosphere and the ocean, Fig. 1 (Jain et al., 1994a; Jain et al., 1995). The model consists of a homogeneous atmosphere, ocean mixed layer and land biosphere boxes, and a vertically-resolved upwelling-diffusion deep ocean. The detailed description of the ocean and biospheric components of this model are given by Jain et al. (1995), and Kheshgi et al. (1996), respectively. In our model, the thermohaline circulation is schematically represented by polar bottom water formation, with the return flow upwelling through the 1-D water column to the surface ocean from where it is returned, through the polar sea, as bottom water to the bottom of the ocean column thereby completing the thermohaline circulation. The response of bottom-water carbon concentration to changes in the mixed-layer concentration is modeled parametrically by the parameter $\pi = 0.5$ as described in detail by

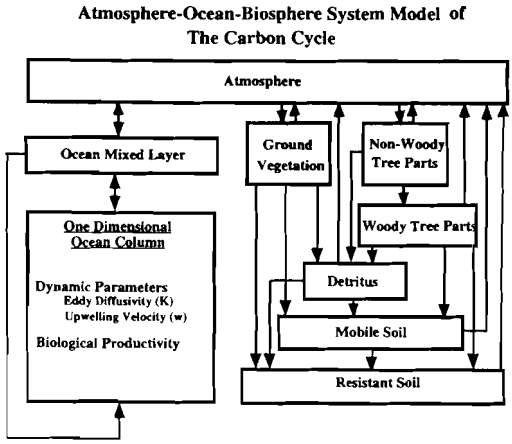

Fig. 1. Schematic diagram of the coupled atmosphere-ocean-biosphere model for the global carbon cycle.

Jain et al. (1995). A marine biosphere source term is included in the deep sea associated with the oxidation of the organic debris exported from the mixed layer where it is produced by photosynthesis (Jain et al., 1995; Volk and Hoffert, 1985). In our model, the surface ocean marine biogenic flux of carbon is 8.5 GtC/yr (Table 1) which lies at the middle of the observed range from 2 to 20 GtC/yr (Sundquist, 1985; Siegenthaler and Sarmiento, 1993).

The two model-ocean dynamic parameters (eddy diffusivity κ, and advection velocity w) are calibrated by matching the natural ^{14}C distribution in the deep ocean. The values of κ and w required to match the pre-industrial, vertical profile of ^{14}C are 4700 m^2/yr and 3.5 m/yr. The carbonate equilibrium in the mixed ocean layer is calculated from the full set of chemical equations as described by Peng et al. (1987).

The global-mean gas-exchange rate at pre-industrial CO_2 concentration of 278 ppm is 17.0 mol/m^2/yr was estimated from the ^{14}C balance of the atmosphere and ocean surface reservoirs (Jain et al., 1995) for the steady state (1765) concentrations listed in Table 1. Our value is slightly lower than that adopted by Hesshaimer et al.(1994) of 17.4 mol/m^2/yr and Broecker and Peng (1994) of 17.8 mol/m^2/yr. Toggweiler et al. (1989) estimated the global-mean gas-exchange rate value of 16.6 mol/m^2/yr which is slightly lower than our estimated value. Our value is also higher than the value of 15.2 mol/m^2/yr obtained by

Table 1. *Values of the parameters used in the global carbon cycle model*

CO_2 concentration in steady state atmosphere	278 ppm
CO_2 mass in steady state atmosphere	590 Gt C
CO_2 biosphere mass in steady state	2327 Gt C
CO_2 mass in steady state mixed layer	676 GT C
Carbon concentration in steady state mixed layer	2.05 mol m^{-3}
Carbon concentration in the steady state polar sea	2.37 mol m^{-3}
total flux of carbon in the surface-ocean layer produced by photoplankton	8.5 GtC yr^{-1}
^{13}C concentration in steady state atmosphere	−6.3‰
^{13}C concentration in steady state mixed layer	1.9‰
^{13}C concentration in steady state polar sea	0.1‰
^{14}C mean production rate from cosmic ray flux	2 atom cm^{-2} s^{-1}
^{14}C concentration in steady state atmosphere	0‰
^{14}C concentration in steady state mixed layer	−50‰
^{14}C concentration in steady state polar sea	−150‰
average depth of the mixed layer	75 m
average depth of the deep ocean	4000 m
ocean surface area	3.62×10^{14} m^2
vertical eddy diffusivity	4700 m^2 yr^{-1}
upwelling velocity	3.5 m yr^{-1}
gas exchange rate at 278 ppm	17.0 (mol m^{-2} yr^{-1})
buffer factor for excess CO_2	variable
decay constant of ^{14}C	1/8267 yr
fertilization factor β	0.39
bottom water surface concentration feedback parameter Π_c	0.5
$^{13}C/^{12}C$ Fractionation factors	
for CO_2 uptake by terrestrial biosphere	0.982
for CO_2 release by terrestrial biosphere	1
for CO_2 uptake by surface ocean	0.998
for CO_2 release from the surface ocean	0.989
for marine biosphere	0.976
$^{14}C/^{12}C$ Fractionation factors	
square of that for $^{13}C/^{12}C$	

Siegenthaler and Joos (1992). It is important to note that our estimated gas exchange rate value is within the range of other model studies.

To estimate terrestrial biospheric fluxes, a six-box globally aggregated terrestrial biosphere submodel is coupled to the atmosphere box (Fig. 1). The terrestrial biosphere model is made up of six boxes which represent ground vegetation, non-woody tree parts, woody tree parts, detritus, mobile soil with a turnover time 70 years, and resistant soil with a turnover time 500 years. The mass of carbon contained in the different reservoirs and their turnover times as well as the rates of exchange between them have been based on the analysis by Harvey (1989) and Kheshgi et al. (1996). The effects of land use are included by changing (decreasing with time) the total productive land area covered by the terrestrial biosphere. The carbon mass in each of the boxes is proportional to the total productive land area. Decreases in area lead to CO_2 emissions due to changes in land use as well as a decrease in the global rate of carbon exchange with the (smaller) biosphere. A simple model representation of biospheric feedbacks to changes in the atmospheric concentration of CO_2 and the global mean-annual near-surface temperature are included. An increase in the rate of net photosynthesis (NP) or net primary productivity (NPP, equal to NP minus respiration by woody tree parts) by terrestrial biota, relative to preindustrial times, is modeled to be proportional to the logarithm of the relative increase in atmospheric CO_2 concentration from its pre-industrial value of 278 parts per million (ppm). The magnitude of the modeled biospheric sink depends primarily on the chosen value of the proportionality constant β known as the CO_2 fertilization factor (Harvey, 1989; Wigley, 1993). The value of

$\beta = 0.39$ used in the current study leads to a reconstruction of the past carbon cycle, described in the next section, which is consistent with a land use emission estimate of 11.0 gigaton of carbon (GtC) for the decade 1980–1989 (IPCC, 1996). In addition, the rate coefficients for exchange to and from terrestrial biosphere boxes (respiration and photosynthesis) vary with global mean annual temperature (which is calculated by an energy balance climate model (Jain et al., 1994b) consistent with the model used by IPCC (IPCC, 1990, 1992, 1996)) according to an Arrhenius law (Harvey, 1989). The mechanism for biospheric feedbacks are not well known, leading to significant uncertainty in the prediction of the behavior of the future carbon cycle. The past net biospheric uptake, however, is constrained by the past carbon budget. We do not expect the past uptake of carbon isotopes to be highly sensitive to the mechanism for biospheric feedback, nor the split between of the net biospheric uptake between emissions from changes in land use or biospheric feedback. If this expectation is true, then isotopic data will have limited use in constraining the cause for changes in biospheric carbon, but rather only the net biospheric sink.

We also include the effects of changes in land use, and a model representation of changes in the metabolism of the terrestrial biosphere in response to changes in the atmospheric environment. Land use emissions are assumed to come from each of the terrestrial biosphere boxes in proportion to the mass of carbon in the box. Photosynthesis and respiration rates are adjusted so that the terrestrial biosphere model will not exhibit regrowth from a previously specified land use emission.

The cycles of ^{13}C and ^{14}C are modeled by additional systems of equations of similar form as for total carbon, except for the inclusion of fractionation, radioactive decay of ^{14}C, and cosmogenic production of ^{14}C. A detailed description of the model equations for the atmosphere, ocean, and terrestrial reservoirs of CO_2 and its isotopes are given by Jain et al. (1995), and Kheshgi et al. (1996). Numerical values of the principal model parameters are given in Table 1. The ^{13}C fractionation coefficients for atmosphere to ocean transfer and vice-versa are adopted from Siegenthaler and Münnich (1981). The ^{13}C fractionation coefficients for terrestrial and marine biospheres are taken from Broecker and Peng(1982) and Keeling et al. (1989). The ^{14}C fractionation coefficients for all processes are simply the square of those for ^{13}C (Keeling, 1981).

In this paper, the ^{13}C concentrations are expressed as $\delta^{13}C$, which is the relative deviation from the *Peedee Belemnite standard* expressed in permil (‰) as

$$\delta^{13}C_i = \left(\frac{[1-(^{13}C/C)_{std}] \times [(^{13}C_i/C_i)/(^{13}C/C)_{std}]}{[1-(^{13}C_i/C_i)]} - 1 \right) \times 1000‰. \quad (1)$$

The ^{14}C concentrations are expressed here in the $\Delta^{14}C$ notation, which is normally defined as the deviation of ^{13}C-normalized concentration from that of the *oxalic acid standard* (at the National Bureau of Standards, USA) expressed in permil (‰) (Stuiver and Pollach, 1977):

$$\Delta^{14}C_i = \left[(1+\delta^{14}C_i)\left(\frac{0.975}{1+\delta^{13}C_i} \right)^2 - 1 \right] \times 1000‰, \quad (2)$$

where

$$\delta^{14}C_i = \frac{(^{14}C_i/C_i)}{(^{14}C/C)_{std}} - 1. \quad (3)$$

However, the observation-based estimates of atmospheric $\Delta^{14}C_i$ (Stuiver and Quay, 1980; Broecker et al., 1985) have been calculated by the approximation of (2) by

$$\Delta^{14}C_i = [\delta^{14}C_i - 2(\delta^{13}C_i + 0.025)(1+\delta^{14}C_i)] \times 1000‰, \quad (4)$$

as originally proposed by Broecker and Olson (1959). We, therefore, have chosen to use (4) to define $\Delta^{14}C_i$ for our model-based estimates.

The mass ratios of the standard's concentrations of ^{13}C and ^{14}C to that of total carbon are (Keeling, 1981):

$$(^{13}C/C)_{std} = 0.0111123,$$

$$(^{14}C/C)_{std} = 1.176 \times 10^{-12}.$$

The mass ratios of ^{13}C and ^{14}C to total carbon in the i'th reservoir are given by $^{13}C_i/C_i$ and $^{14}C_i/C_i$. The model also takes into account the effects of radioactive decay. The radioactive decay constant for ^{14}C is $\lambda = 1.21 \times 10^{-4}$ yr^{-1} (Table 1), whereas it is zero for the stable isotopes ^{12}C and ^{13}C.

3. Reconstruction of anthropogenic effects on the past carbon budget

Estimates of the history of CO_2 emissions (measured in GtC/yr) from the burning of fossil fuels $E_{\text{fossil fuel}}$ are greater than the sum of the modeled uptake of carbon by the oceans plus the observed accumulation of carbon (in the form of CO_2) in the atmosphere. In an attempt to balance the carbon budget we attribute the difference to the net uptake of carbon by the terrestrial biosphere (Siegenthaler and Oeschger, 1987; Wigley, 1993; Enting et al., 1994).

To reconstruct the past carbon budget, we calculate the history of land use emissions from

$$-\frac{dN_b}{dt}=\frac{dN_a}{dt}+\frac{dN_o}{dt}-E_{\text{fossil fuel}}, \quad (5)$$

$$\frac{dN_b}{dt}=S_{\text{biospheric feedbacks}}-E_{\text{land use}}. \quad (6)$$

The observed record of CO_2 concentration from the Siple ice-core (Friedli et al., 1986), and from atmospheric measurements at the Mauna Loa Observatory in Hawaii (Neftel et al., 1985; Keeling et al., 1995), smoothed by a spline fit (Fig. 2), is used to calculate the rate of change dN_a/dt of the carbon mass in the atmosphere. The estimate of the global emission rate $E_{\text{fossil fuel}}$ of CO_2 by the burning of fossil fuels given by Marland et al. (1994) is shown in Fig. 3. The ocean carbon cycle model described in the previous section (Jain et al., 1995) is used to calculate the rate of accumulation dN_o/dt of mass of carbon N_o in the oceans with the atmospheric concentration of CO_2 specified to be the spline fit to the observed record. The net uptake of carbon by the terrestrial biosphere dN_b/dt is calculated from eq. (5). Land use emissions are then calculated from the rate of uptake of carbon by terrestrial biosphere feedbacks $S_{\text{biospheric feedback}}$ (calculated in response to the spline fit to the observed history of atmospheric CO_2 (spline fit) using the approach in the model description given in the previous section (Kheshgi et al., 1996)) and dN_b/dt by eq. (6). In this way the modeled carbon cycle is forced to replicate the smoothed history of atmospheric CO_2 concentration. A similar approach was used by the IPCC (IPCC, 1996) to reconstruct the past carbon budget.

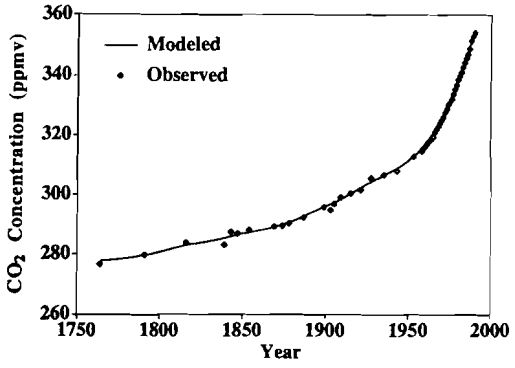

Fig. 2. Observed atmospheric CO_2 increase from 1765 to 1990. The observed data from 1765 to 1954 is from the Siple ice-core record (Neftel et al., 1985; Friedli et al., 1986) and thereafter it is from the Mauna Loa Observatory, Hawaii (Keeling et al., 1995). The continuous line is a spline fit through the observed data which is specified as the atmospheric concentration in the model, and has been used to estimate the emission rate of carbon dioxide from land use changes by eq. (5).

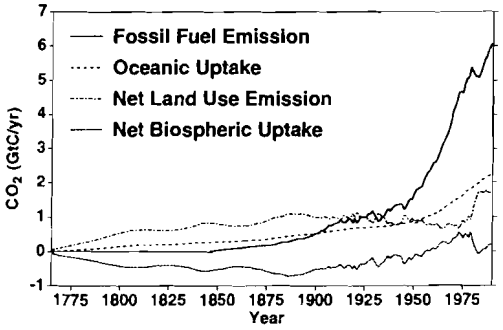

Fig. 3. Model-estimated CO_2 fluxes for terrestrial biosphere (net land use emissions and net biospheric uptake) and ocean reservoirs obtained from the deconvolution of the observed CO_2 record shown in Fig. 1. The fossil fuel CO_2 emissions are taken from Marland et al. (1994).

The curves for oceanic and net biospheric uptakes shown in Fig. 3 closely resemble those presented by the IPCC (IPCC, 1996). In Fig. 3, land use emissions $E_{\text{land use}}$ are larger than $E_{\text{fossil fuel}}$ in 19th century, while the reverse is seen in the 20th century where there has been a rapid increase in fossil fuel emissions. After 1890, a slow increase of net terrestrial biospheric uptake occurs up to 1975, followed by rapid decline and then a increase starting in the early 1980s. This increase is presumably due to fluctuations in $E_{\text{fossil fuel}}$ that was not picked up in the smoothed atmospheric CO_2

record. Fig. 3 also shows a continuous increase of oceanic uptake over the period 1765–1990. Our model estimated carbon budget over the period 1980–1989 as shown in Table 2 is well within the range of estimates summarized by the IPCC (IPCC, 1996).

The past reconstruction of the ^{13}C and ^{14}C cycles are created based on the reconstruction for total carbon summarized in Fig. 3 and Table 2. We start from a model steady state determined by the parameters listed in Table 1. The calculated initial atmosphere (1765), and oceanic concentrations of $\delta^{13}C$ and $\Delta^{14}C$ are given in Table 1. The ^{13}C steady state is determined by the fractionation coefficients and the exchanges of total carbon. The radiocarbon steady state adds the effects of a cosmic radiation source of radiocarbon in the atmosphere and decay of radiocarbon in all the carbon reservoirs (Jain et al., 1995). The changes in atmospheric ^{14}C could also be caused by changes in ^{14}C production rates which are correlated to the sunspot index (Stuiver and Quay, 1980). Because of the uncertainty in the variation of production rate of ^{14}C and its negligible effect on ^{14}C ratio (Bacastow and Keeling, 1973) over the time scale of 100 years (1850–1950), we do not account for this effect in our calculations and thus assume constant cosmic ^{14}C production. The mean production rate of ^{14}C from cosmic rays is taken to be equal to 2 atoms cm^{-2} s^{-1} (Suess, 1955; Craig, 1957). More recently O'Brien (1979) and Stuiver and Quay (1980) also calculated the ^{14}C production rates. O'Brien (1979) estimated cosmogenic production rate over the period 1937–1970. His estimated production rate values vary between 1.88 and 2.12 atoms cm^{-2} s^{-1}. Stuiver and Quay (1980) calculated the mean ^{14}C production rate from neutron flux and sunspot index measurements of 1.88 ± 0.38 atoms cm^{-2} s^{-1} over the period from 1868 to 1967. However, when the sunspot index is assumed zero, the estimated mean ^{14}C production rates of O'Brien (1979) and Stuiver and Quay (1980) are approximately 2.0 atoms cm^{-2} s^{-1}, consistent with the value used in this study.

The time evolution of $\delta^{13}C$ in the atmosphere, oceans and biosphere is calculated with the addition of information on the $\delta^{13}C$ history of fossil fuel emissions. For $\delta^{13}C$ of fossil fuel emissions from 1850 to 1950 we use the estimates given by Tans(1981a). After 1950 we use the estimates given by Andres et al. (1993) which is based on updated

Table 2. *Model reconstruction of the past carbon budget for the periods 1765–1989 and 1980–1989*

	Model-estimated carbon budget		IPCC (1996)[f]
	1765 to 1989	1980 to 1989	1980 to 1989
fossil fuel emissions[a]	212.847 Gt C	54.594 Gt C	55 ± 5 Gt C
atmospheric accumulation[b]	158.967 Gt C	32.797 Gt C	33 ± 2 Gt C
modeled ocean accumulation	118.995 Gt C	19.70 Gt C	20 ± 8 Gt C
net biosphere accumulation[c]	−65.114 Gt C	2.093 Gt C	
modeled biosphere feedback[d]	79.277 Gt C	13.094 Gt C	13 ± 15 Gt C[g]
land use emissions[e]	144.391 Gt C	11.001 Gt C[d]	11 ± 11 Gt C[h]

[a] Fossil fuel taken from Marland et al. (1994).

[b] Atmospheric accumulation is calculated from the changes in atmospheric CO_2 concentration measured from the Siple ice core (Neftel et al., 1985; Friedli et al., 1986) and at the Mauna Loa Observatory (Keeling et al., 1995) over the time periods listed in the Table.

[c] Net biospheric accumulation calculated by subtraction.

[d] The magnitude of the modeled biospheric feedback is adjusted by choice of β to result in 11. Gt C land use emissions for the time period 1980–1989.

[e] Land use emissions calculated by subtraction.

[f] Error limits correspond to an estimated 90% confidence interval.

[g] A net biospheric sink due to CO_2 fertilization (5–20 Gt), nitrogen fertilization (2–10 Gt C) and climatic effects (0–10 Gt C).

[h] This is a sum of net emissions from changes in tropical land use (16 ± 10 Gt C) and the carbon sink due to Northern Hemisphere forest regrowth (5 ± 5 Gt C).

fossil and cement production data (Marland et al., 1994). The estimated value of $\delta^{13}C$ in 1990 is $-28‰$, which is 4‰ less than the estimated 1850 value of $-24‰$. Prior to 1850, we assume that the $\delta^{13}C$ of fossil fuel emissions is equal to the 1850 estimate.

Prior to 1950, the time evolution of $\Delta^{14}C$ in the atmosphere, oceans and biosphere is calculated. After 1950, above-ground testing of nuclear weapons led to a source of radiocarbon in the atmosphere. The rate of bomb-production of radiocarbon, however, is not well known. In this study we prescribe the average observed atmospheric $\Delta^{14}C$ after 1950 (Tans, 1981b; Broecker and Peng, 1994, and the references cited therein), calculate the response of $\Delta^{14}C$ in the oceans and biosphere, and infer the bomb-^{14}C production rate from the rate of change of the atmosphere/oceans/biosphere inventory of ^{14}C.

In the following sections we compare our model estimates of isotopic concentrations in different carbon reservoirs with the observed data.

4. The evolution of atmospheric ^{13}C and ^{14}C

Changes in atmospheric $\delta^{13}C$ and $\Delta^{14}C$ match the modeled responses of atmospheric composition to the emissions of fossil fuel biospheric carbon as shown in Fig. 4 and summarized in Table 3.

The carbon in fossil fuels and the terrestrial biosphere have $\delta^{13}C$ values of roughly $-25‰$ compared to the atmospheric $\delta^{13}C$ of roughly $-7‰$ (Friedli et al., 1986); therefore, the transfer of either fossil or biospheric carbon to the atmosphere reduces the atmospheric $\delta^{13}C$. The observed $\delta^{13}C$ data shown in Fig. 4a from 1765 to 1953, and also for the year 1980, are from $\delta^{13}C$ measurements of air trapped in ice from Siple station (Friedli et al., 1986). Data for the year 1956 and for the period 1978 through 1990 are from direct measurement of atmospheric $\delta^{13}C$ at the Mauna Loa Observatory (Keeling et al., 1979; Keeling et al., 1989; Keeling et al., 1995). The accelerating decrease of $\delta^{13}C$ is caused in the model system by the increasing fossil fuel plus net biospheric emissions shown in Fig. 3. Measurements by Keeling et al. (1979, 1980, 1989) and Mook et al. (1983) show that the $\delta^{13}C$ has decreased from $-6.79‰$ in 1956 to $-7.34‰$ in 1978 and to $-7.68‰$ in 1988. Together the data summarized in Fig. 4a indicate that the $\delta^{13}C$ of atmospheric CO_2 has decreased by 1.46‰ from 1765 to 1988 which is consistent with our model estimated $\delta^{13}C$ change of 1.48‰. Separately, the ice core data from 1800 to 1980 and the Mauna Loa data from 1956 to 1988 show $\delta^{13}C$ decreases of $1.14 \pm 0.15‰$ and $0.89 \pm 0.13‰$ which are consistent with our model estimated decreases of 1.27‰ and 0.85‰ for the these two periods (see Table 3).

The dilution of $\Delta^{14}C$, know as the Suess effect (Suess, 1955), is apparent in measured atmospheric ^{14}C before 1950 (Fig. 4b), after which $\Delta^{14}C$ increases drastically due to radiocarbon produced by above-ground nuclear weapons tests. This dilution effect is mainly due to the emission of ^{14}C-free CO_2 from the burning of fossil fuels, which lowers the atmospheric $\Delta^{14}C$. Emissions (or exchange) of CO_2 from the above ground reservoirs of carbon have a ^{14}C ratio nearly the same as the atmospheric ratios. The soil reservoirs, on the other hand, have a very slow exchange with the atmosphere, although they have a lower value of $\Delta^{14}C$ due to radiocarbon decay of the old carbon. Therefore, compared to the fossil-CO_2 emission, the emission and exchange of carbon between the terrestrial biosphere and the atmosphere is expected to have a small effect on the atmospheric ^{14}C ratio.

By measurement of $\Delta^{14}C$ in tree-rings representing the period 1840 through 1950, Stuiver and Quay (1981) found a reduction in atmospheric $\Delta^{14}C$ of $-20 \pm 4‰$ (see Table 3 and Fig. 4(b)) and Keeling (1973) found a $-25‰$ effect; our model-estimated effect on atmospheric $\Delta^{14}C$ over this time period was $-20‰$ (see Table 3). Our model estimated atmospheric $\Delta^{14}C$ from 1840 to 1950 are shown in Fig. 4b to be consistent with tree ring data (Stuiver and Quay, 1981).

Fig. 4b shows the modeled evolution of $\Delta^{14}C$ from 1950 to 1990, if we neglect the bomb-production of radiocarbon and continue to calculate the atmospheric $\Delta^{14}C$. In the absence of bomb production, the model estimates an atmospheric change of $\Delta^{14}C$ from 1950 to 1990 is $-50‰$. Of course, in reality, there is significant bomb-production of radiocarbon in the atmosphere after 1950, which we consider in Section 6.

Table 3. *Comparison of global carbon cycle model results with observations*

	Model	Observation
Atmospheric $\Delta\delta^{13}C$ (‰)		
1800 to 1980	−1.27	-1.14 ± 0.15[a]
1956 to 1988	−0.85	-0.89 ± 0.15[b]
Mixed Layer $\Delta\delta^{13}C$ (‰)		
1800 to 1970	−0.52	-0.45 ± 0.05[c]
1970 to 1990	−0.35	−0.39[d]
$\Delta\delta^{13}C$ Ocean Inventories (‰ m)		
1970 to 1990	−150	-208 ± 45[d]
$\Delta\delta^{13}C$ Penetration Depth (m)		
1970 to 1990	432	520 ± 115[d]
Atmospheric $\Delta\ ^{14}C$ (‰)		
1840 to 1950	−20	-20 ± 4[e]
Mixed Layer $\Delta^{14}C$ (‰)		
1850 to 1950	−6.6	-9 ± 3[f]
Bomb ^{14}C Inventories (10^{13} atoms/m^2)	9.0	8.5 ± 0.9[g]
Bomb ^{14}C penetration depth (m)	308	328 ± 30[g]

[a] Ice core measurements (Friedli et al. 1986).
[b] Mauna Loa measurements (Keeling et al., 1979, 1980, 1989).
[c] Measurements for Berumuda Coral (Nozaki et al., 1978; Druffel and Benavides, 1986).
[d] Global estimate (Quay et al. 1992).
[e] Tree ring data (Stuiver and Quay, 1981).
[f] Radiocarbon measurements for Pacific and Atlantic corals (Druffel and Linick, 1978; Druffel and Suess, 1983).
[g] Estimates based on GEOSECS data (Broecker et al., 1995)

5. The evolution of ^{13}C and ^{14}C in the surface waters of the oceans

Changes in atmospheric $\delta^{13}C$ and $\Delta^{14}C$ are modeled to cause changes in the isotopic composition of the ocean mixed layer.

Analyses of Bermuda coral by Nozaki et al. (1978) and Druffel and Benavides (1986) indicate a $\delta^{13}C$ decrease in the ocean mixed layer of -0.45 ± 0.05‰ from 1800 to 1970 as compared to our model result of −0.52‰ (Table 3). Our $\delta^{13}C$ decrease for the ocean mixed layer of -35‰ from 1970 to 1990 are somewhat lower than the recent estimates of −39‰ obtained by Quay et al. (1992) over the same period (Table 3). A possible explanation for the difference is the fact that the Quay et al. estimates are based on Pacific Ocean data and do not include $\delta^{13}C$ data from the Indian and Atlantic oceans. Druffel and Linick (1978) and Druffel and Suess (1983) measured a change of -9 ± 3‰ in the ocean mixed layer $\Delta^{14}C$ over the period 1850–1950. This estimate is based on the average of the radiocarbon measurements for Pacific and Atlantic corals which includes, for example, Florida coral (-11‰), Belize coral (-12‰), and Galapagos coral (-6‰). Our carbon cycle model predicts a mixed layer decline of −6.6‰ over the same period (Table 3).

6. Oceanic dissolved inorganic carbon, ^{13}C and ^{14}C at the time of GEOSECS

A primary motivation for using tracers to calibrate ocean carbon cycle models is the difficulty of estimating from direct measurements the net uptake of carbon dioxide by the oceans, or the net accumulation of carbon in the oceans. The pre-industrial radiocarbon has been used to calibrate ocean-carbon cycle model parameters, in particular for the ocean-atmospheric exchange coefficients (Broecker et al., 1985) and ocean mixing parameters (Oeschger et al., 1975; Jain et al., 1995). To test the dynamic model response, we compare our model results to the measured values of oceanic dissolved inorganic carbon (DIC), the $\delta^{13}C$ of DIC, and bomb-produced radiocarbon in DIC. The requirement that a model reproduce these tracers further constrains the

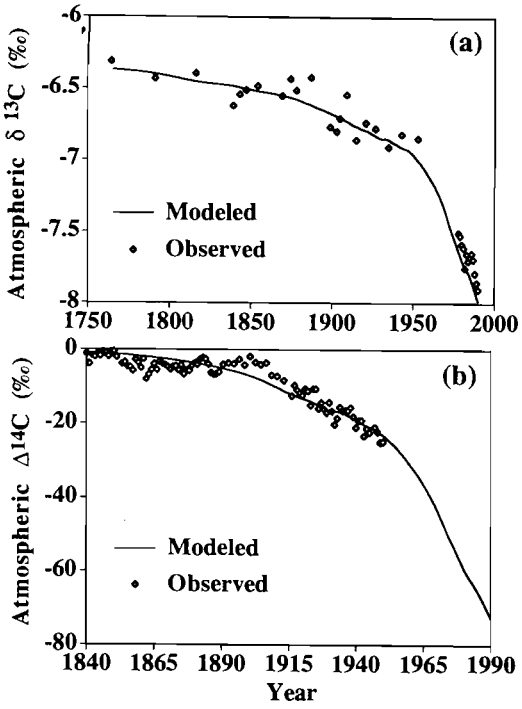

Fig. 4. (a) Model estimate of the dilution of atmospheric ^{13}C by the burning of fossil-fuels and land use changes is compared to the observation data. Data from 1765 to 1950 is from ^{13}C measurements of air trapped in ice from Siple Station (Friedli et al., 1986). Data from 1978 to 1990 is from direct measurements of atmospheric ^{13}C at the Mauna Loa Observatory (Keeling et al., 1979, 1989, 1995). (b) Model estimate of the dilution of atmospheric ^{14}C by the burning of fossil-fuels and land use changes is compared to tree ring measurements of Stuiver and Quay (1981) from 1840 to 1950. This comparison ends in 1950 due to onset of nuclear testing. This figure also shows the expected dilution of the atmospheric $^{14}C/C$ ratio from 1950 to 1990 in the absence of nuclear testing.

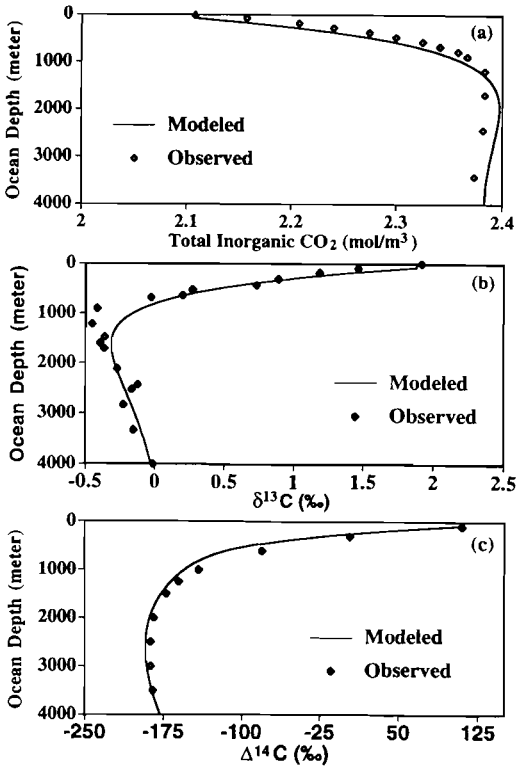

Fig. 5 Comparison of the model-estimated (a) total inorganic carbon (mol/m3) (b) ^{13}C of dissolved inorganic carbon (‰) and (c) bomb-produced ^{14}C (‰) in the ocean with the observed data. The observed data in Figs. 5a, b, c are global averages of the GEOSECS data taken from Takahashi et al. (1981), Kroopnick (1985), and Shaffer and Sarmiento (1995), respectively.

model response over decadal time scales (Broecker et al., 1985; Kheshgi et al., 1995).

Variations in the concentration of dissolved inorganic carbon with depth are controlled by several processes: vertical mixing, the rate of production of particulate organic carbon in the mixed layer (ocean net primary production), and the depth profile at which settling particulate organic carbon (POC) is respired and released as dissolved inorganic carbon (Kheshgi et al., 1991). Note that this model takes into account first two processes only. In Fig. 5a, the model-estimated depth profile of DIC at the beginning of 1975 is compared with the GEOSECS-derived data of Takahashi et al. (1981) intended to be applicable for that time. The model-estimated surface ocean DIC concentration of 2.11 mol/m^3 is close to the GEOSECS-derived value of 2.09 mol/m^3(Takahashi et al., 1981). The observed concentration of DIC increases as one descends from the surface to reach a maximum at about 1000 m and then decreases toward the ocean floor. The consistency of the depth profile of DIC generated by the model, which contains an upwelling/diffusion model for vertical mixing and an exponential depth profile for the release of inorganic carbon from the settling particulate organic carbon, to the GEOSECS-based data shows that the modeled processes are sufficient to reproduce this behavior.

The $\delta^{13}C$ of DIC provides a further constraint

on the carbon cycle and helps us understand the invasion of fossil fuel CO_2 into the main thermocline. Carbon isotopes are fractionated during dissolution in sea water, the production of organic matter, and the formation of $CaCO_3$ (see Table 1 for fractionation coefficients). The variation of the $\delta^{13}C$ of $\sum CO_2$ can be used to evaluate the relative importance of the vertical mixing of DIC and the transport of carbon by the settling of POC. Fig. 5b shows the comparison of the observed GEOSECS depth profile of $\delta^{13}C$ of DIC with the modeled values. The $\delta^{13}C$ decreases with depth as the DIC maximum zone ($\approx$900 m) is approached because of the addition of isotopically light CO_2 from the respiration of POC (McNichol and Druffel, 1992). Below this zone, mixing with isotopically heavier bottom water causes $\delta^{13}C$ to increase (Kroopnick, 1985). Fig. 5b shows that the model-estimated depth profile for the year 1974 is consistent with the GEOSECS observed data. The model-estimated surface ocean $\delta^{13}C$ concentration was 1.87‰ compared to the GEOSECS measured value of 2.0‰ (Kroopnick, 1985).

The bomb-^{14}C tracer is used to examine mixing processes capable of removing ^{14}C (or CO_2) from the atmosphere on a decade time-scale. This is in contrast to the pre-industrial distribution of ^{14}C, which was used to calibrate the ocean mixing parameters κ and w, and is sensitive to slow mixing processes ($\approx$500 yr) approaching the half-life time of radiocarbon (5730 yr). Since the rate of ^{14}C produced by nuclear weapon tests is not precisely known, the global-mean-annual atmospheric $\Delta^{14}C$ derived from observations and listed by Tans, (1981b) and Broecker and Peng (1994) are prescribed from 1950 to 1990. The model estimate is compared in Fig. 5c to the observed depth profile of $\Delta^{14}C$ in the ocean for the GEOSECS year 1974 constructed by Shaffer and Sarmiento (1995). Bomb-produced ^{14}C causes the high values of $\Delta^{14}C$ above the thermocline (at depth less than 1000 m). While the model slightly underestimates the $\Delta^{14}C$ near the thermocline, elsewhere the model is able to reproduced the observed bomb ^{14}C distribution.

In order to quantify the amount of anthropogenic CO_2 taken up by the oceans, we have also estimated the depth-integrated changes and the mean penetration depth of change in the ocean $\Delta^{14}C$ and $\delta^{13}C$ as defined by Broecker et al. (1985), Quay et al. (1992), and Jain et al. (1995).

The observed estimated changes in the depth-integrated $\delta^{13}C$ and the penetration depth between 1970 to 1990 were -208 ± 45‰ m and 520 ± 115 m, based on $\delta^{13}C$ measurements in the Pacific Ocean and the ocean-wide extrapolation with the use of the bomb ^{14}C burden, as discussed by Quay et al. (1992). Our model-estimated values of depth-integrated $\delta^{13}C$ and the penetration depth are -150‰ m and 432 m for the period 1970–1990. Table 3 shows that our model-estimated value of penetration depth is within the range of uncertainty of the observation-based estimate. However, the model-estimated value of depth-integrated $\delta^{13}C$ is outside the estimated range of uncertainty of the observation-based value. While there are differences between model and observed values, we feel that the uncertainty in the globally-averaged depth-integrated $\delta^{13}C$ value based on observations is greater than estimated by Quay et al. (1992), considering the very limited amount of data; uncertainties could be reduced by continued oceanic $\delta^{13}C$ measurements.

The change in the ocean inventory and the implied penetration depth of bomb-^{14}C estimated by Broecker et al. (1995) from 1950 to the nominal GEOSECS year of 1974 are $8.5 \pm 0.9 \times 10^{13}$ atoms/m^2 and 328 ± 30 m, respectively (see Table 3). Our model-estimated bomb-^{14}C inventory of 9.0×10^{13} atoms/m^2 and the penetration depth of 308 m are about 6% higher and 7% lower, respectively, than the observation-based estimates. Note that the parameter values of κ and w are able to reproduce the ocean inventory of bomb-produced ^{14}C even though the values were calibrated to match the natural ^{14}C oceanic distribution.

7. Closure of the global budget of bomb radiocarbon

Two recent studies (Broecker and Peng, 1994; Hesshaimer et al., 1994) have found that their model-estimated growth of global inventory of radiocarbon does not balance the independently estimated rate of radiocarbon production from nuclear weapons tests. Hesshaimer et al. (1994) attributed this imbalance to the overestimation of about 25% in the amount of the ocean uptake of ^{14}C at the time of GEOSECS survey (Broecker et al., 1985). Broecker and Peng (1994) suggested

that the imbalance in the bomb ^{14}C budget might be due to undetected ^{14}C concentrations in the stratosphere, or error in the model estimated change of the ocean inventory with time. Joos (1994) compared the three different model-estimated changes (Hesshaimer et al., 1994; Broecker and Peng, 1994; Siegenthaler and Joos, 1992) in bomb ^{14}C inventories for mid-1965 to mid-1989 with the known bomb ^{14}C sources and concluded that the model-estimated global inventories are about 10–15% higher compared to the total bomb ^{14}C production. More recently, Broecker et al. (1995) have re-revised the observed estimates of global ocean bomb ^{14}C inventories for the GEOSECS time period (1972–1978), giving values consistent with their earlier estimates (Broecker et al, 1985). Based on an ocean carbon cycle model calibrated to the re-revised estimates of observed ocean ^{14}C inventory, Broecker et al. (1995) were able to account for all the bomb ^{14}C within the limits of uncertainty. Duffy and Caldeira (1995), using an ocean general circulation tracer model have also estimated the bomb ^{14}C budget and reached conclusions similar to those of Broecker et al. (1995).

In Table 4, we have compared our model-estimated bomb ^{14}C inventories for stratosphere, troposphere, biosphere, and ocean reservoirs, and the bomb ^{14}C production between mid-1965 and mid-1989 with other model results. The estimated results for the model of Siegenthaler and Joos (1992) are taken from Joos (1994). The estimated results for Broecker et al. (1995) are taken from their fig. 18. Broecker and Peng (1994) and Broecker et al. (1995) provided their models' inventories for January 1 of the year. In order to get the mid-year value, we have simply taken the average of consecutive years.

Comparison of the change in ocean inventory of radiocarbon for the period 1965 to 1989 estimated by different studies, as summarized in Table 4, shows that our model-estimated ocean inventory is within $\pm 10\%$ of other estimates, with the exception of Broecker and Peng (1994). We believe the uncertainty of our estimate (90% confidence interval) to be equal to the proposed $\pm 10\%$ uncertainty of the data-based estimate of bomb-radiocarbon ocean inventory on 1 January by Broecker et al. (1995); a heuristic argument for this uncertainty is that both the data-based estimate (1950 to 1975) and other data constraints (e.g. the depth profile of radiocarbon in the oceans) are used to reduce the uncertainty of our estimate over the different time period (1965 to 1990). Our model-estimated value of $286 \pm 29 \times 10^{26}$ atoms is about 13% lower than the estimate of Broecker and Peng (1994). This difference is due to the fact that Broecker and Peng (1994) calibrated their model to give a bomb-radiocarbon ocean-inventory on 1 January, 1974 of 370×10^{26} atoms,

Table 4. *Comparison of model-estimated changes in bomb ^{14}C inventories between mid-1965 and mid-1989 with other model results and the bomb ^{14}C production; the units are 10^{26} atoms of bomb ^{14}C*

Bomb-^{14}C inventories and production	This study	Hesshaimer et al. (1994)	Broecker & Peng (1994)	Broecker et al. (1995)	Sigenthaler & Joos (1992)	Duffy & Caldeira (1995)
ocean[a]	286 ± 29	299	322	300	287	268
biosphere[a]	92 ± 37	60	37	37	99	
troposphere[a]	-148 ± 15	-150				
stratosphere[b]	-117 ± 24	-100				
total inventory[c]	113 ± 55	109				
bomb ^{14}C-production	56 ± 28	55				
net imbalance[c]	58 ± 62	54				

[a] The ocean, biosphere and troposphere inventories are calculated from the observed tropospheric ^{14}C ratios and model calculated CO_2 concentrations.

[b] The stratospheric values are from Duffy et al. (1995), which matches the observed data for the period 1963–1969 (Telgadas, 1971).

[c] Uncertainties estimated by quadratic error addition.

which is about 20% higher than their re-revised inventory of 305×10^{26} atoms. Broecker et al. (1995) later recalibrated their model based on the re-revised data-based ocean inventory, and then estimated the change in ocean inventory of radiocarbon for the period 1965 to 1990 to be 300×10^{26} atoms (value taken from their figure 18), which is only 5% higher than our estimate.

Biospheric inventories of bomb-^{14}C are quite uncertain, because there are no accurate data-based estimates of bomb-^{14}C inventories that can be used to calibrate or constrain model processes. We assume that uncertainty (90% confidence interval) in the biospheric estimates of radiocarbon inventory is 40%, as did Joos (1994). The biospheric inventory estimates between mid-1965 and mid-1989 of five model studies shown in Table 4, range from 37 to 99×10^{26} atoms. Our model estimated bomb-14C inventory for the terrestrial biosphere over the same period (1965–1990) of $92 \pm 37 \times 10^{26}$ atoms is within our range of uncertainty of other estimates.

The tropospheric inventory used in our carbon budget is calculated from the measured Δ^{14}C (Tans, 1981b; Broecker and Peng, 1994; and the references cited therein) and model estimated δ^{13}C, δ^{14}C and atmospheric CO_2 content which is taken to be 85% of the total atmospheric CO_2 content (which is proportional to the spline fit to CO_2 data shown in Fig 2). The estimated uncertainty in tropospheric ^{14}C inventories between 1965 and 1990 was of the order of $\pm 10\%$ (Joos, 1994) which is also assumed in this study. The estimated tropospheric inventory for the period 1965–1990 is $-148 \pm 15 \times 10^{26}$ atoms, which is slightly lower than the Hesshaimer et al. (1994) estimate of 150×10^{26} atoms.

The stratospheric inventory, adopted from Duffy et al. (1995), is calculated by our two dimensional (latitude and altitude) chemical-radiative-transport model of the global atmosphere (Wuebbles et al., 1991; Kinnison et al., 1994). Unlike Hesshaimer et al. (1994) and Broecker and Peng (1994), the modeled stratospheric residence time of bomb-^{14}C is dependent on the magnitudes of the stratospheric circulation, which is derived from first principles. The time-dependent lower boundary values specified by the model were obtained from data by Johnston (1989). The ^{14}C concentration and the resultant inventory are calculated by prescribing the ^{14}C input from the atmospheric bomb tests, which is based on the compilation of bomb strength data (Hesshaimer et al., 1994, and the references provided therein). The model also takes into account bomb-^{14}C production created by the nuclear tests created in the atmosphere during 1965–1989. The model estimated ^{14}C concentrations in the troposphere and stratosphere, as well as stratospheric inventory compare well with the observed data in the analyses by Telegadas, (1971) and Johnston (1989) (Kinnison et al., 1994). The model stratospheric inventory corresponds to the 15% of the stratospheric mass. The ^{14}C results of this model have also been compared in assessment studies to other two and three dimensional models (Prather and Remsberg, 1993) and are representative of current understanding of stratospheric processes.

The observed stratospheric calculations of Telegadas (1971) are based on aircraft and balloon data. However, as noticed by Tans (1981), these aircraft and balloon data cannot be calibrated with the ground-based collection. The Telegadas (1971) estimates of tropospheric input of bomb ^{14}C are, on average, 20% higher than the tropospheric estimates made from ground-based CO_2 collections, as well as when they are compared to high altitude measurements by Ergin et al. (1970). Broecker and Peng (1994) and Broecker et al. (1995) suggest that inconsistency in the global bomb radiocarbon inventory might be due to stratospheric radiocarbon missed in the measurements. We assume that the stratospheric inventory estimates are good to within $\pm 20\%$ (90% confidence limit). Our model-estimated change in stratospheric radiocarbon inventory between mid-1965 and mid-1989 is $-117 \pm 23 \times 10^{26}$ atoms compared to the Hesshaimer et al. (1994) estimate of -110×10^{26} atoms.

In the present study, the cumulative production of bomb-^{14}C for the period 1965–1989 is estimated from bomb strength data (compiled in units of megatons, Mt, TNT by Hesshaimer et al., 1994), and by adopting a constant cumulative bomb-^{14}C production per Mt TNT parameter that will match to global change in modeled ^{14}C inventory (sum of stratosphere, troposphere, biosphere, and ocean inventories) during the period 1950–1963 of intense nuclear weapons testing as seen in Fig. 6. Fig. 6 also shows that after 1963 our estimated combined inventory exceed the estimated production of bomb ^{14}C. The estimated combined invent-

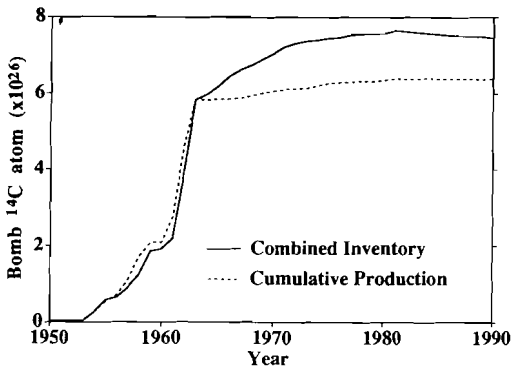

Fig. 6. Estimated total bomb ^{14}C inventories and the cumulative productions as a function of time. The total bomb ^{14}C inventories are the sum of troposphere, stratosphere, terrestrial biosphere, and ocean inventories. Cumulative production matches the total inventories in the year 1963.

ory, as of 1990 was 740×10^{26} atoms compared to cumulative bomb ^{14}C production of 640×10^{26} atoms. The uncertainty in current estimates of bomb-^{14}C production could, however, be as large as 50% (based on private communication with R. Lougheed of Lawrence Livermore National Laboratory, also see Wuebbles, 1995) because the amounts of radionuclides generated by different bomb tests are not well known. Although, various estimates exist in the literature for the characteristics of individual tests (Bauer, 1979), there does not exist a database that brings together all of the information on these tests and the radionuclides produced. The estimated cumulative production between mid-1965 and mid-1989 in this study is taken to be $56 \pm 28 \times 10^{26}$ atoms compared to the Hesshaimer et al. (1994) estimate of $55 \pm 22 \times 10^{26}$ atoms.

Table 4 shows that our model-estimated bomb ^{14}C budget imbalance for the period 1965–1989 was $58 \pm 69 \times 10^{26}$ atoms which is approximately the same as previously calculated by Hesshaimer et al. (1994). However, the imbalance is well within the range of our hypothesized uncertainties. Our analyses suggest that there is no need to revise the global ocean inventories, but rather develop an inventory of radionuclide production (and characteristics) from atmospheric nuclear tests, and evaluate the utility of this inventory in support of modeling of global atmospheric and oceanic processes. These analyses and modeling studies will provide meaningful tests and validation of the capabilities of carbon cycle models.

8. Model impulse responses: CO_2, ^{13}C and ^{14}C

The response of a model atmosphere to an impulse of CO_2 to the atmosphere can be used to characterize the behavior of the global carbon cycle model (Enting et al., 1994; Kheshgi et al., 1996; Kheshgi and White, 1996). The impulse response function is also required to determine the Global Warming Potential (GWP) that characterizes the relative measure of the potential effects on climate from various gas emissions as compared to CO_2 (IPCC, 1990, 1996). Furthermore, the response to an impulse of radiocarbon has been used to further describe the carbon cycle system (Broecker and Peng, 1982; Siegenthaler and Oeschger, 1987; Joos et al., 1996), although there has been some confusion as to the interpretation of this information (IPCC, 1996).

Fig. 7 shows the time-responses of the model atmospheric concentration to small impulses of CO_2, ^{14}C and ^{13}C to the atmosphere. The impulse response curves have been calculated by adding a small amount of CO_2 into an atmosphere with steady-state CO_2, ^{14}C and ^{13}C concentrations (identical to the 1765 atmosphere estimated from

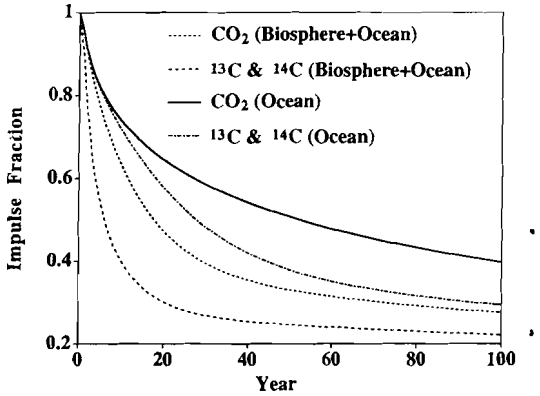

Fig. 7. Model-estimated atmospheric response to a pulse input of CO_2 and $\delta^{13}C$ and $\Delta^{14}C$. In addition to the ocean, the terrestrial biosphere and the soil will also absorb the carbon. Therefore, the figure shows the response to a pulse input with and without biospheric reservoirs. The amount of pulse was injected into a pre-industrial constant atmosphere.

the values listed in Table 1), integrating forward and calculating the concentration differences from the constant background case. The impulse response curves shown in Fig. 7 are normalized to the size of the impulse; therefore, the impulse response has a value of one at time $t=0$. The impulse responses for ^{14}C and ^{13}C are not visibly different in the figure. When a pulse of CO_2, ^{14}C or ^{13}C is added to the atmosphere, a fractions of the pulse are take up by the terrestrial biosphere and by the oceans. In order to differentiate the effects of the oceans and the terrestrial biosphere, results are shown for two different incarnations of the model. For the responses labeled "ocean", the model does not contain a biosphere which exchanges carbon with the atmosphere for each of the impulses. For the responses labeled "ocean + biosphere", the model contains an interactive biosphere. The impulse response for CO_2 decreases due to dissolution of a fraction of the impulse in the ocean, and the incorporation of a fraction of the impulse in the organic carbon of the model plants and soils. The biospheric uptake is a consequence of modeled biospheric feedbacks to increasing CO_2 concentration by a CO_2 fertilization effect and a dependence of photosynthesis/respiration on global-mean temperature (which depends on CO_2 concentration). The CO_2 response also depends on the background CO_2 concentration (in this case it is a constant 278 ppm), as has been studied in detail by Kheshgi et al. (1996).

The impulse response for the isotopes (^{14}C and ^{13}C) is, according to the model mechanisms, different than for CO_2. For the case with no biosphere, the isotope response initially declines at nearly the same rate as the CO_2 impulse. This is because the initial rate of impulse dissolution of both CO_2 and the isotopes are limited by air/sea exchange by virtually the same extent. At a later time, the ocean-fraction of the isotope impulse exceeds that of the CO_2 impulse, and ultimately leads to a larger ocean fraction for the isotopes. This is because, in equilibrium, a change in the isotopic concentration in the oceans corresponds to a similar relative change in the atmospheric concentration; whereas, a change in the total carbon concentration in the oceans corresponds to a much larger relative change in the partial pressure of CO_2 in sea water (by an amount equal to the differential buffer factor) and, correspondingly, to a much larger relative change in atmospheric concentration of CO_2.

There is a quite large difference between the runs with and without a biosphere, demonstrating the importance of the terrestrial biosphere for the carbon cycle. For the case with an interactive biosphere, the isotope biospheric fraction of the impulse increases more rapidly than that for CO_2, even at short times. This is because a primary limit to isotope uptake is the mixing (or turnover) of carbon into the biospheric carbon reservoirs, until the reservoirs contain an isotopic ratio (to total carbon) roughly equal to that of the atmosphere. The biospheric uptake of CO_2, however, is controlled by the modeled biospheric feedbacks, and not the turnover of carbon directly. For example, if the two biospheric feedbacks of CO_2 fertilization and the dependence of photosynthesis/respiration on global-mean temperature were turned off, the biospheric fraction of a CO_2 impulse would be zero (Kheshgi et al., 1996), whereas there would still be isotopic uptake due to the turnover of biospheric carbon of different composition than the atmosphere. Use of model response to impulses of carbon isotopes as a model diagnostic may well have potential.

9. Conclusions

A carbon cycle model describing the exchange of carbon between the atmosphere, ocean and terrestrial biosphere has been applied to estimate the isotopic anomaly in the atmosphere, the ocean and the biosphere. This model for the carbon cycle is constructed to be consistent with our understanding of the global carbon cycle. Validation of the capability of the model to represent this understanding is partially based on the analysis of tracer records such as those for ^{13}C and ^{14}C; therefore, in addition to reproducing the past record of CO_2 concentration, it is important that a carbon cycle model also be able to reproduce tracer records. Different tracers are sensitive to different components of the model. For example, the modeled absorption of CO_2 by the oceans is closely related to the ocean inventory of bomb-produced ^{14}C from atmospheric nuclear testing in the 1950s and early 1960s. The past variation of ^{13}C is related to the emission or uptake of CO_2 by the terrestrial biosphere and fossil fuel burning, because of the

significant isotopic fractionation of terrestrial biospheric and fossil fuel carbon which occurs during photosynthesis. Our model is found to match measured values, within the uncertainty range, of the pre-bomb decrease in ^{14}C in the atmosphere and the mixed layer due to the Suess Effect, the bomb-^{14}C in the ocean, the bomb-^{14}C ocean inventory, and the vertical distribution of total carbon. At the same time, the model-calculated atmospheric $^{13}C/^{12}C$ trend, based on the CO_2 concentration record, agrees well with the observed ice core and tree-ring record. The model has also been used to estimate the $^{13}C/^{12}C$ of oceanic dissolved inorganic carbon, and our model results have been found to match observations well within the range of observational uncertainty. Our confidence in both experimental techniques and our understanding of the global carbon cycle is strengthened by the consistency between carbon isotopes concentration data and model results.

REFERENCES

Andres, R. J., Marland, G. and Bischof, S. 1996. The carbon dioxide emissions from fossil fuel combustion and cement manufacture 1751–1991 and an estimate of their isotopic composition and latitudinal distribution. In: *The carbon cycle*, ed. T. M. Wigley. Cambridge University Press, in press.

Bacastow, R. and Keeling, C. D. 1973. Atmospheric carbon dioxide and radiocarbon on the natural carbon cycle. In: *Carbon and the biosphere*, ed. G. M. Woodwell and E. V. Pecan, pp. 86–135, US Atomic Energy Commission.

Bauer, E. 1979. A catalog of perturbing influences on stratospheric ozone, 1955–1975. *J. Geophys. Res.* **84**, 6929–6940.

Broecker, W. C. and Olson, E. A. 1959. Lamont radiocarbon measurements VI. *American Journal of Science Radiocarbon Supplement* **1**, 111–132.

Broecker, W. S. and Peng, T.-H. 1994. Stratospheric contribution to the global bomb radiocarbon inventory: model versus observation. *Global Biogeochemical Cycles* **8**, 377–384.

Broecker, W. S., Peng, T.-H. and Engh, R. 1980. Modeling the carbon system. *Radiocarbon* **22**, 565–580.

Broecker, W. S., Peng, T.-H., Ostlund, G. and Stuiver, M. 1985. The distribution of bomb radiocarbon in the ocean. *J. Geophys. Res.* **90**, 6953–6970.

Broecker, W. S. and Peng, T. H. 1982. *Tracers in the sea.* Eldegio Press, Lamont-Doherty Geological Observatory. 691 pp.

Broecker, W. S., Sutherland, S., Smethie, W., Peng, T.-H. and Ostlund, G. 1995. Oceanic radiocarbon: Separation of the natural and bomb components. *Global Biogeochemical Cycles* **9**, 263–288.

Cias, P., Tans, P. P., Trolier, M., White, J. W. C. and Francey, R. J. 1995. A large Northern Hemisphere terrestrial CO_2 sink indicated by the $^{13}C/^{12}C$ ratio of atmospheric CO_2. *Science* **269**, 1098–1102.

Craig, H. 1957. The Natural distribution of radiocarbon and the exchange time of carbon dioxide between atmosphere and sea. *Tellus* **9**, 1–17.

Druffel, E. M. and Benavides, L. M. 1986. Input of excess CO_2 to the surface ocean based on $^{13}C/^{12}C$ ratios in a banded Jamaican sclerosponge. *Nature* **321**, 58–61.

Druffel, E. M. and Linick, T. W. 1978. Radiocarbon in annual coral rings of Florida. *Geophys. Res. Let.* **5**, 913–916.

Druffel, E. M. and Suess, H. E. 1983. On the radiocarbon record in banded corals. *Geophys. Res. Let.* **88**, 1271–1280.

Duffy, P., and Caldeira, K. 1995. Three dimensional model calculation of ocean uptake of bomb ^{14}C and implications for the global budget of bomb ^{14}C. *Global Biogeochemical Cycles* **9**, 373–375.

Duffy, P., Amthor, J. C., Caldeira, K., Connell, P., Kinnison, D. E., Southon, J. and Wuebbles, D. J. 1995. *The global budget of bomb radiocarbon.* Lawrence Livermore National Laboratory, UCRL-JC-120675, National Technical Information Service, US Dept. of Commerce, 5285 Port Royal Rd, Springfield, VA 2261, USA.

Enting, I. G. and Pearman, G. I. 1987. Description of a one-dimensional carbon cycle model calibrated by the techniques of constrained inversion. *Tellus* **39B**, 459–476.

Enting, I. G., Wigley, T. M. L. and Heimann, M., Eds. 1994. *Future emissions and concentrations of carbon dioxide: key ocean/atmosphere/land analyses,* 120 pp. Australia, CSIRO, 1994.

Ergin, M., Harkeness, D. D. and Walton, A. 1970. Uppsala radiocarbon measurements X. *Radiocarbon* **12**, 281–284.

Friedli, H., Lotscher, H., Oeschger, H., Siegenthaler, U. and Stauffer, B. 1986. Ice core record of the $^{13}C/^{12}C$ ratio of atmospheric carbon dioxide in the past two centuries. *Nature* **324**, 237–238.

Harvey, L. D. D. 1989. Effect of model structure on the response of terrestrial biosphere models to CO_2 and temperature increases. *Global Biogeochemical Cycles* **3**, 137–153.

Hesshaimer, V., Heimann, M. and Levin, I. 1994. Radiocarbon evidence for a smaller ocean carbon dioxide sink than previously believed. *Nature* **370**, 201–203.

Intergovernmental Panel on Climate Change (IPCC). 1990. *Climate change: the IPCC scientific assessment*, eds. Houghton, J. T., Jenkins, G. J., and Ephraums, J. J. Cambridge University Press, Cambridge.

IPCC (Intergovernmental Panel on Climate Change). 1992. *Climate change 1992, The supplementary report to the IPCC scientific assessment*, eds. Houghton, J. T., Callander, B. A., and Varney, S. K. Cambridge University Press, Cambridge.

IPCC (Intergovernmental Panel on Climate Change). 1996. Climate change 1995, the science of climate change, eds. Houghton, J. T., Meira Filho, L. G., Callander, B. A., Harris, N., Kattenberg, A. and Maskell, K. Cambridge University Press.

Jain, A. K., Kheshgi, H. S., Caldeira, K., Hoffert, M. I. and Wuebbles, D. J. 1994a. Evaluation of $\delta^{13}C$ of atmospheric carbon dioxide with a schematic carbon cycle model. *American Geophysical Union Fall Meeting, EOS Supplement* **75**, 152–153.

Jain, A. K., Kheshgi, H. S. and Wuebbles, D. J. 1994b. *Integrated science model for assessment of climate change*. 94-TP59. 08, Air and Waste Management Association, also Lawrence Livermore National Laboratory, UCRL-JC-116526, National Technical Information Service, US Dept. of Commerce, 5285 Port Royal Rd, Springfield, VA 2261.

Jain, A. K., Kheshgi, H. S., Hoffert, M. I. and Wuebbles, D. J. 1995. Distribution of radiocarbon as a test of global carbon cycle models. *Global Biogeochemical Cycles* **9**, 153–166.

Johnston, H. S. 1989. Evaluation of excess carbon 14 and strontium 90 data for suitability to test two-dimensional stratospheric models, *J. Geophys. Res.* **94**, 18485–18493.

Joos, F. 1994. Imbalance in the budget. *Nature* **370**, 181–182.

Joos, F., Bruno, M., Fink, R., Siegenthaler, U., Stocker, T., Le Quere, C. and Sarmiento, J. L. 1996. An efficient and accurate representation of complex oceanic and biospheric models of anthropogenic carbon uptake. *Tellus* **48**, (in press).

Keeling, C. D. 1973. The carbon dioxide cycle: Reservoir models to depict the exchange of atmospheric carbon dioxide with the oceans and land plants. In: *Chemistry of the lower atmosphere*, ed. S. I. Rasool, pp. 251–329. Plenum.

Keeling, C. D., Bacastow, R. B., Carter, A. F., Piper, S. C., Whorf, T. P., M. Heimann, Mook, W. G. and Roeloffzen, H. 1989. A three-dimensional model of atmospheric CO_2 transport based on observed winds. 1. Analysis of observational data. In: *Aspects of climate variability in the Pacific and Western Americas*, ed. D. H. Peterson, pp. 165–236. Am. Geophys. Union.

Keeling, C. D., Bacastow, R. B. and Tans, P. 1980. Predicted shift in the $^{13}C/^{12}C$ ratio of atmospheric carbon dioxide. *Geophys. Res. Let.* **7**, 505–508.

Keeling, C. D., Mook, W. G. and Tans, P. 1979. Recent trends in the $^{13}C/^{12}C$ ratio of atmospheric carbon dioxide. *Nature* **277**, 121–123.

Keeling, C. D., Whorf, T. P., Wahlen, M. and Pilcht, J. V. D. 1995. Interannual extremes in the rates of rise of atmospheric carbon dioxide since 1980. *Nature* **375**, 666–670.

Kheshgi, H. S., Hoffert, M. I. and Flannery, B. P. 1991. Marine biota effects on the compositional structure of the world oceans. *J. Geophys. Res.* **96**, 4957–4969.

Kheshgi, H. S., Jain, A. K. and Wuebbles, D. J. 1996. Accounting for the missing carbon sink with the CO_2 fertilization effect. *Climatic Change* **33**, 31–62.

Kheshgi, H. S., Jain, A. K. and Wuebbles, D. J. 1995. Uncertainty in the global carbon budget derived from isotopic constraints, American Geophys. Union Fall Meeting, EOS Suppl. 76, F83.

Kheshgi, H. S. and White, B. S. 1996. Modeling ocean carbon cycle with a nonlinear convolution model. *Tellus* **48B**, 3–12.

Kinnison, D. E., Johnston, H. S. and Wuebbles, D. J. 1994. Model study of atmospheric transport using carbon 14 and strontium as inert tracers. *J. Geophys. Res.* **99**, 20647–20664.

Kroopnick, P. M. 1985. The distribution of ^{13}C of $\sum CO_2$ in the world oceans. *Deep-Sea Research* **32**, 57–84.

Maier-Reimer, E. 1993. Geochemical tracers in an ocean general circulation model. Preindustrial tracer distributions. *Global Biogeochemical Cycles* **7**, 645–677.

Maier-Reimer, E. and Hasselmann, K. 1987. Transport and storage of CO_2 in the ocean. An inorganic ocean-circulation carbon cycle model. *Clim. Dyn.* **2**, 63–90.

Marland, G., Andres, R. J., and Boden, T. A. 1994. Global, regional, and national CO_2 emissions. In: *Trends 93: A compendium of data on global change*, ed. Boden, T. A., Kaiser, D. P., Sepanski, R. J. and Stoss, F. W., pp 505–584. Oak Ridge Natl. Lab, Oak Ridge, Tenn., USA, ORNL/CDIAC-65.

McNichol, A. P. and Druffel, E. R. M. 1992. Variability of the $\delta^{13}C$ of dissolved inorganic carbon at a site in the north Pacific Ocean. *Geochemica et Cosmochimica Acta* **56**, 3589–3592.

Mook, W. G., Koopmans, M., Carter, A. F. and Keeking, C. D. 1983. Seasonal Latitudinal and secular variations in the abundance and isotopic ratios of atmospheric carbon dioxide. *J. Geophys. Res.* **88**, 10915–10933.

Neftel, A., Moor, E., Oeschger, H. and Stauffer, B. 1985. Evidence from polar ice cores for the increase in atmospheric CO_2 in the past two centuries. *Nature* **315**, 45–47.

Nozaki, Y., Rye, D. M., Turekian, K. K., Dodge, R. E. 1978. A 200 year record of carbon-13 and carbon-14 variations in a Bermuda coral. *Geophys. Res. Let.* **5**, 825–828.

O'Brien, K. 1979. Secular variations in the production of cosmogenic isotopes in the Earth's atmosphere. *J. Geophys. Res.* **84**, 423–431.

Oeschger, H., Siegenthaler, U., Schotterer, U. and Guglemann, A. 1975. A box-diffusion model to study

the carbon dioxide exchange in nature. *Tellus* **27**, 168–192.

Peng, T.-H., Takahashi, T., Broecker, W. S. and Olafsson, J. 1987. Seasonal variability of carbon dioxide, nutrients and oxygen in the northern North Atlantic surface water. *Tellus* **39B**, 439–458.

Prather, M. J., and Remsberg, E. E. 1993. *The atmospheric effects of stratospheric aircraft.* Report of the 1992 Models and Measurement Workshop (3 volumes). NASA Ref. Publ. 1292.

Quay, P. D., Tilbrook, B. and Wong, C. S. 1992. Oceanic uptake of fossil fuel CO_2: Carbon-13 evidence. *Science* **256**, 74–79.

Sarmiento, J. L., Orr, J. C. and Siegenthaler, U. 1992. A perturbation simulation of CO_2 uptake in an ocean general circulation model. *J. Geophys. Res.* **97**, 3621–3645.

Shaffer, G. and Sarmiento, J. L. 1995. Biogeochemical cycling in the global ocean 1: A new, analytical model with continuous vertical resolution and high latitude dynamics. *J. Geophys. Res.* **100**, 2659–2672.

Siegenthaler, U. and Joos, F. 1992. Use of a simple model for studying oceanic tracer distributions and the global carbon cycle. *Tellus* **44B**, 186–207.

Siegenthaler, U. and Münnich, K. O. 1981.$^{13}C/^{12}C$ fractionation during CO_2 transfer from air to sea. In: *Carbon Cycle Modeling, SCOPE 16,* ed. B. Bolin, pp. 249–257. John Wiley & Sons.

Siegenthaler, U. and Oeschger, H. 1987. Biospheric CO_2 emissions during the past 200 years reconstructed by deconvolution of ice core data. *Tellus* **39B**, 140–154.

Siegenthaler, U. and Sarmiento, J. L. 1993. Atmospheric carbon dioxide and ocean. *Nature* **365**, 119–125.

Stuiver, M. and Pollach, H. 1977. Discussion reporting of ^{14}C data. *Radiocarbon* **19**, 355–363.

Stuiver, M. and Quay, P. D. 1980. Changes in atmospheric ^{14}C attributed to variable sun. *Science* **207**, 11–19.

Stuiver, M. and Quay, P. D. 1981. Atmospheric ^{14}C changes resulting from fossil fuel CO_2 release and cosmic ray flux variability. *Earth Planet. Sci. Lett.* **53**, 349–362.

Suess, H. E. 1955. Radiocarbon concentration in modern wood. *Science* **122**, 415–417.

Sundquist, E. T. 1985. Geological perspectives on carbon dioxide and the carbon cycle. In: *The carbon cycle and atmospheric CO_2: natural variations archean to present. Geophysical Monograph* **32**, eds. Sundquist, E. T. and Broecker, W. S. American Geophysical Union, Washington D. C.

Takahashi, T., Broecker, W. S. and Bainbridge, A. E. 1981. Supplement to the alkalinity and total carbon dioxide concentration in the world oceans. In: *Carbon cycle modeling, SCOPE 16,* ed. B. Bolin, pp. 159–200. John Wiley & Sons.

Tans, P. 1981a.$^{13}C/^{12}C$ of industrial CO_2. In: *Carbon cycle modeling, SCOPE 16,* ed. B. Bolin, pp. 127–129. John Wiley & Sons.

Tans, P. P. 1981b. A compilation of bomb ^{14}C data for use in global carbon cycle models. In: *Carbon cycle modeling, Scope 16,* ed. B. Bolin, pp. 131–158. John Wiley & Sons.

Tans, P. P., Fung, I. Y. and Takahashi, T. 1990. Observational constraints on the global atmospheric CO_2 budget. *Science* **247**, 1431–1438.

Telegadas, K. 1971. *The seasonal atmospheric distribution and inventories of excess ^{14}C from March 1955 to July 1969.* Health and Safety Lab., US At. Energy Comm., Washington, D.C., Rep. 243.

Toggweiler, J. R., Dixon, K. and Bryan, K. 1989. Simulations of radiocarbon in a coarse resolution world ocean model (I). Distributions of bomb-produced ^{14}C. *J. Geophys. Res.* **94**, 8243–8264.

Volk, T. and Hoffert, M. I. 1985. Ocean carbon pumps: analysis of relative strengths and efficiencies in ocean-driven atmospheric CO_2 changes. In: *The carbon cycle and atmospheric CO_2: natural variations archean to present. Geophysical Monograph* **32**, pp. 91–110, American Geophysical Union, Washington, DC.

Wigley, T. M. L. 1993. Balancing the carbon budget. Implications for projections of future carbon dioxide concentration changes. *Tellus* **45B**, 409–425.

Wuebbles, D. J., D. E. Kinnison, K. E. Grant, and J. Lean. 1991. The effect of solar flux variations and trace gas emissions on recent trends in stratospheric ozone and temperature. *J. Geomagnetism and Geoelectricity,* **43**, 709–718.

Wuebbles, D. J. 1995. *Utility of past atmospheric nuclear test data in global climate change research. The need for new analyses,* produced for the US Department of Energy, USA, internal report, Dept. of Atmospheric Science, University of Illinois, Urbana, IL 61801.